The University of Nottingham
UNITED KINGDOM · CHINA · MALAYSIA

Arjmand, Elaheh and Agyakwa, Pearl A. and Corfield, Martin R. and Li, Jianfeng and Mouawad, Bassem and Mark Johnson, C. (2016) A thermal cycling reliability study of ultrasonically bonded copper wires. Microelectronics Reliability, 59 . pp. 126-133. ISSN 0026-2714

Access from the University of Nottingham repository:
http://eprints.nottingham.ac.uk/37320/1/1-s2.0-S0026271416300099-main.pdf

Copyright and reuse:

The Nottingham ePrints service makes this work by researchers of the University of Nottingham available open access under the following conditions.

This article is made available under the Creative Commons Attribution licence and may be reused according to the conditions of the licence. For more details see: http://creativecommons.org/licenses/by/2.5/

A note on versions:

The version presented here may differ from the published version or from the version of record. If you wish to cite this item you are advised to consult the publisher's version. Please see the repository url above for details on accessing the published version and note that access may require a subscription.

For more information, please contact eprints@nottingham.ac.uk

Microelectronics Reliability 59 (2016) 126–133

Contents lists available at ScienceDirect

Microelectronics Reliability

journal homepage: www.elsevier.com/locate/mr

A thermal cycling reliability study of ultrasonically bonded copper wires

Elaheh Arjmand *, Pearl A. Agyakwa, Martin R. Corfield, Jianfeng Li, Bassem Mouawad, C. Mark Johnson

Department of Electrical & Electronic Engineering, The University of Nottingham, University Park, Nottingham NG7 2RD, UK

ARTICLE INFO

Article history:
Received 22 May 2015
Received in revised form 18 November 2015
Accepted 16 January 2016
Available online 25 January 2016

Keywords:
Heavy copper wire bonding
Reliability
Power electronics
Passive thermal cycling
Hardness

ABSTRACT

In this work we report on a reliability investigation regarding heavy copper wires ultrasonically bonded onto active braze copper substrates. The results obtained from both a non-destructive approach using 3D X-ray tomography and shear tests showed no discernible degradation or wear out from initial conditions to 2900 passive thermal cycles from −55 to 125 °C. Instead, an apparent increase in shear strength is observed as the number of thermal cycles increases. Nanoindentation hardness investigations suggest the occurrence of cyclic hardening. Microstructural investigations of the interfacial morphologies before and after cycling and after shear testing are also presented and discussed.

© 2016 The Authors. Published by Elsevier Ltd. This is an open access article under the CC BY license (http://creativecommons.org/licenses/by/4.0/).

1. Introduction

In advanced and novel applications of power electronic modules, modules must be designed and manufactured to be capable of achieving higher switching frequencies and thus higher junction temperatures [1]. Current packaging and assembly technologies require further optimization and improvement to find reliable packaging solutions [2]. Failure analysis reveals that wire bond interconnections and solder joints are perhaps the most important life-limiting areas in power electronic modules [3–6]. New packaging and assembly technologies can address these issues by modification of wire bonding and solder joint materials [2,7]. It has been suggested that Al wire bonds might be replaced by copper wire bonds [8,9] and solder joints replaced by low temperature silver sintering or diffusion soldering [10]. However, replacing existing technologies with new ones presents new challenges [11,12].

The recent interest in employing copper wire for interconnections instead of aluminium wire in semiconductor packaging is driven by a number of anticipated advantages [6]. Copper wire offers higher electrical and thermal conductivity compared to aluminium wire, and this may facilitate the achievement of higher current densities. It also has higher yield strength and mechanical stability which is expected to have a positive effect on thermo-mechanical reliability of wire bonds [4]. Table 1 shows a brief comparison of material properties between aluminium wire and copper wire.

Notwithstanding the abovementioned advantages, copper bonding suffers from some limitations. Copper wire is much harder compared to aluminium, so a higher bonding force and a higher value of ultrasonic power are required, and these can potentially damage the bond pad; this applies to either copper metallized die or copper substrates [11]. Furthermore, copper oxide easily forms at room temperature, and this can lead to poor bonding and a constant need to modify bonding parameters and set-up [11]. So far, indications are that copper wire bond reliability supersedes that of Al [4]; however, the mechanisms and modes by which copper bonds fail and the process parameters needed to achieve a reliable production process are still not well understood. In this paper, we characterise the reliability behaviour of copper wires bonded onto active braze copper substrates. Our aim is to attempt to elucidate the degradation behaviour of copper bonds.

2. Experimental procedures

99.99% pure annealed copper wires, 381 μm (0.015″) in diameter, were ultrasonically bonded on a F&K Delvotec ultrasonic wedge–wedge bonder at room temperature onto active metal brazed copper (AMB Cu) substrates with following bonding parameters: Time 300 ms; Ultrasonic power 165 digits; Bond force starts 600 cN; Bond force ends 1100 cN; Touchdown steps: 100 μm (see Fig. 1). The AMB Cu substrates consist of 300 μm top plate and 250 μm under plate layers of 99.95% pure copper on 1 mm thick aluminium nitride ceramic. A Versa-XRM500 microCT system supplied by Carl Zeiss X-ray Microscopy was used for a same-sample X-ray tomography study. Four bonds were randomly selected for X-ray tomography and imaged in the as-bonded condition and then after 900, 1300, 2100 and 2900 cycles, respectively. The pixel size was kept fixed at 1.73 μm for all datasets. The bonds were subjected to passive thermal cycling from −55 to +125 °C in an environmental chamber. A limited number of bonds were selected for shear testing and the remaining bonds were examined by tweezer pull-test after every 100 cycles in order to determine the occurrence of any lift-offs or failures. Optical microscopy, scanning electron

* Corresponding author.
E-mail address: eexea8@nottingham.ac.uk (E. Arjmand).

http://dx.doi.org/10.1016/j.microrel.2016.01.009
0026-2714/© 2016 The Authors. Published by Elsevier Ltd. This is an open access article under the CC BY license (http://creativecommons.org/licenses/by/4.0/).

Table 1
Material properties of aluminium vs. copper [13].

Material properties	Aluminium	Copper
Thermal conductivity	~218 W/m·K	~399 W/m·K
CTE	23.6 ppm	17.7 ppm
Yield strength	29 MPa	140 MPa
Melting point	660.3 °C	1083 °C
Elastic modulus	69 GPa	110–128 GPa
Electrical resistivity	2.68 μOhm·cm	1.72 μOhm·cm

microscopy (SEM) and focused ion beam (FIB) ion channelling of polished cross-sections were used to evaluate the bond pad area and characterise the bond interface microstructures. These were prepared by mounting the samples in edge-retentive epoxy resin and curing at room temperature for 24 hours. This was followed by successive grinding with 1200, 2500 and 4000 grit silicon carbide papers, and 3 μm and 1 μm diamond slurries on a Buehler Metaserv automatic polisher. Etched microstructures were achieved by a final vibrational polish in a 0.06 μm colloidal silica suspension. Room temperature nanoindentation of polished cross-sections was performed using a CSM NHT2 machine platform equipped with a Berkovich indenter with a 50 nm tip radius. Indentation arrays were made which ran parallel to the bond interface and spanned both the wire and substrate. The indent spacing was set at 42 μm. The indentation tests were performed at a maximum load of 10 mN with a 10 s dwell at maximum load, and at a constant loading and unloading rate of 0.167 mN/s. Indentation hardness values were extracted from the load–displacement curves using the Oliver & Pharr method [14].

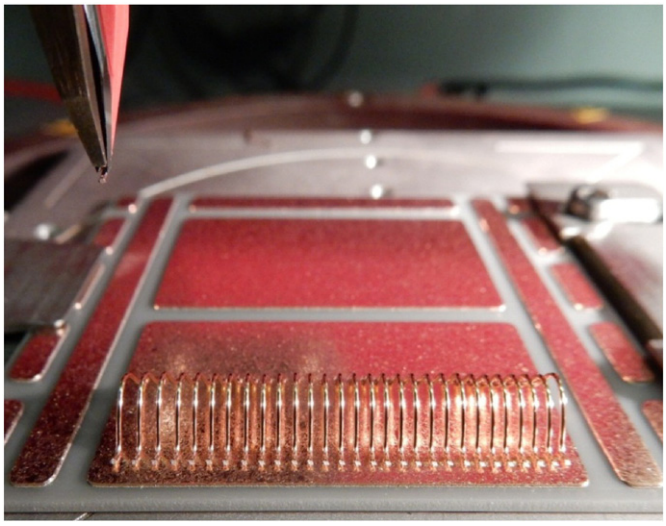

Fig. 1. Copper wires bonded onto AMB cu substrate.

3. Results and discussions

3.1. 3D X-Ray tomography analyses

Four bonds were randomly selected for tomography as can be seen in Fig. 2.

The bonds were imaged at zero cycles (i.e. the as-bonded condition) in order to provide information about initial bond conditions. The bonds were then subjected to thermal cycling between −55 to 125 °C and the same bonds were repeatedly imaged at 1300 cycles, 2100 cycles and 2900 cycles. Virtual cross-sections in the X–Y (lateral) plane of two different bonds are shown in Fig. 3.

These same cross-sections of the interface were analysed at each imaging stage. The arrows in Fig. 3 show some initial pre-cracked regions, mainly in rising heel and tail regions of the bonds. Apart from pre-cracks the bond interfaces seem free of damage in the initial condition, and the bond interfaces do not show any further sign of damage as the number of cycles increases. Interestingly, the analysis of images in the Y–Z plane (as given in Fig. 4) show initial pre-cracks underneath the wire interface, which are not parallel but propagate through the substrate at a 45 degree angle; this is most evident in Bond 2. In addition, no further degradation can be seen as the number of cycles increases (see Fig. 4). Thus far, no lift-offs have been observed.

3.2. Shear test results and microstructural characterisation

Shear testing was also undertaken to determine any changes at the bond interfaces. During the shear test, a shear tool applies a horizontal force to the wire bond to push it off. 24 bonds in total were randomly selected for shear test at zero cycles and then after thermal cycling. Mean values of maximum shear force are presented below in Fig. 5. It is remarkable to note that the average shear force apparently increases with increasing number of cycles: an increase of 25% was observed after 2900 cycles.

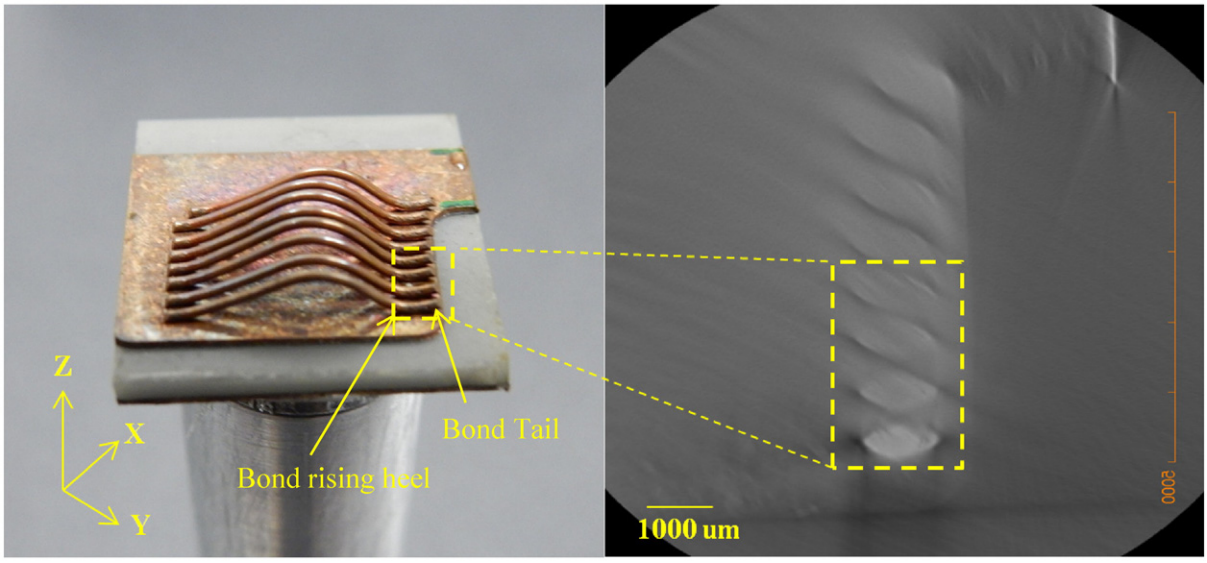

Fig. 2. Selected copper bonds for tomography.

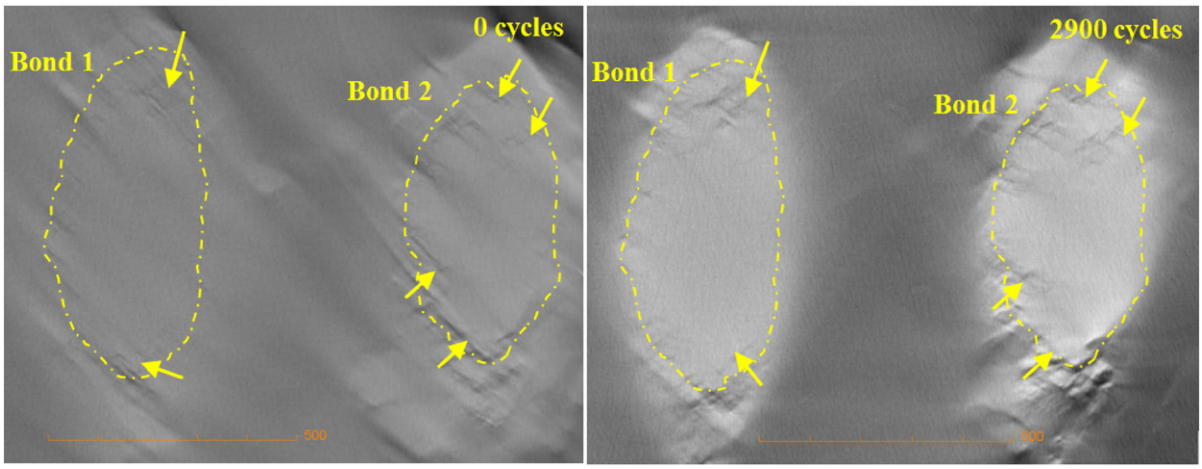

Fig. 3. X-ray tomography images of the first two bonds in X–Y plane.

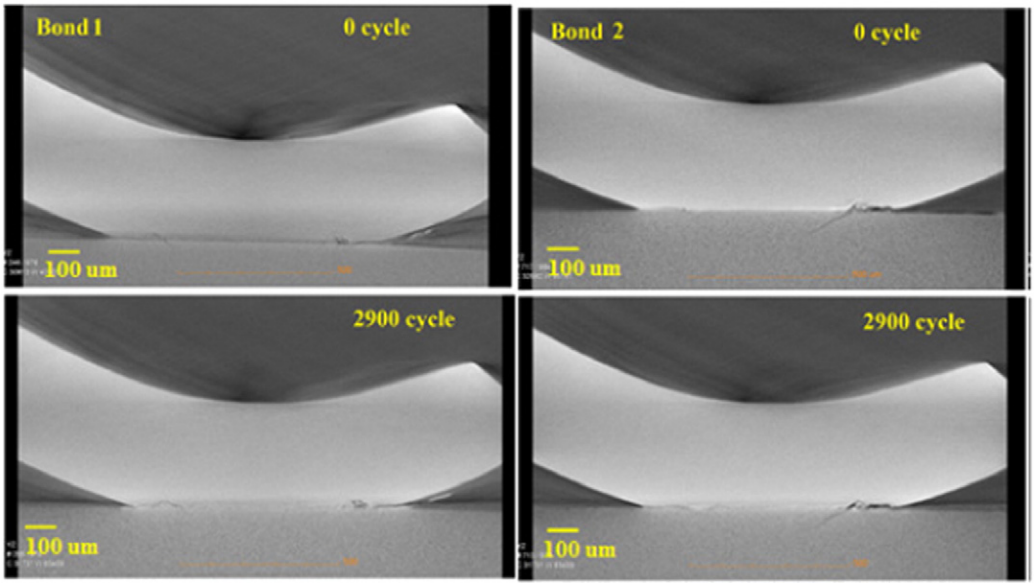

Fig. 4. Virtual cross-sections of two different bonds in Y–Z plane showing damage at zero cycles, and 2900 cycles (same sample study).

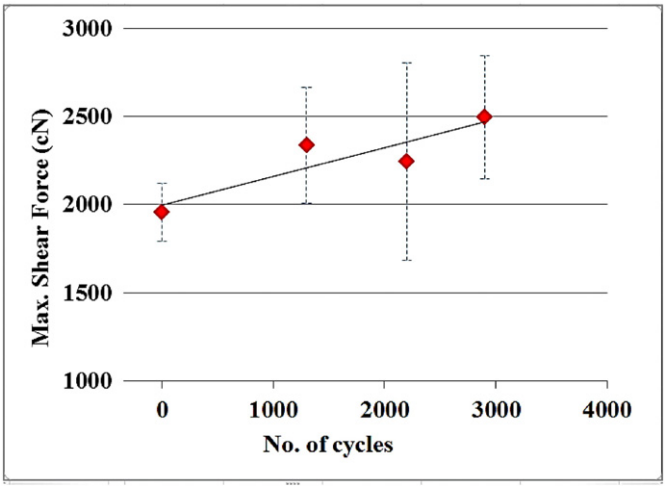

Fig. 5. Shear strength results of copper bonds.

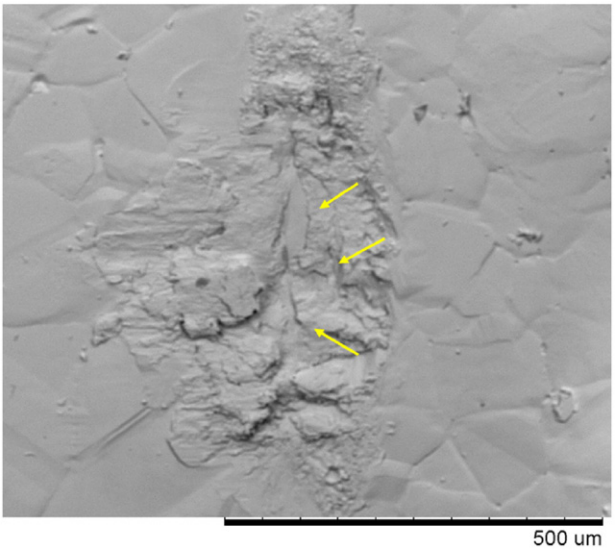

Fig. 6. Fracture surface of bond sheared area in the as-bonded condition.

Scanning electron microscopy was used to observe the bond interfaces after shear test. The topography of the fracture surfaces consistently revealed craters or hollows in the substrate material immediately beneath the bonds (see Fig. 6), consistent with shear code C2 as described in MILSTD883. The surfaces also revealed the existence of copper-rich spheroidal particles containing some copper oxide at both extremities of bonds, as can be seen in Fig. 7-a, b, e and f. In addition to these observations, the shear surface exhibits copper grains elongated in the axis of the shear direction; this would indicate a ductile mode of fracture (see Fig. 7-d).

In order to explain the interfacial particles and the seemingly anomalous increase in shear strength, metallurgical cross-sections were prepared and characterised via optical microscopy, FIB ion channelling and nanoindentation. In Fig. 8, optical cross-sections of an as-bonded wire and a cycled wire (after 2900 cycles) are presented in as-polished and etched conditions. It should be noted that these are two different samples. From these images, the direction of the pre-existing cracks previously observed in the tomography images can be seen with greater clarity, and is particularly obvious in the etched images, see Fig. 8(a2) and (b2).

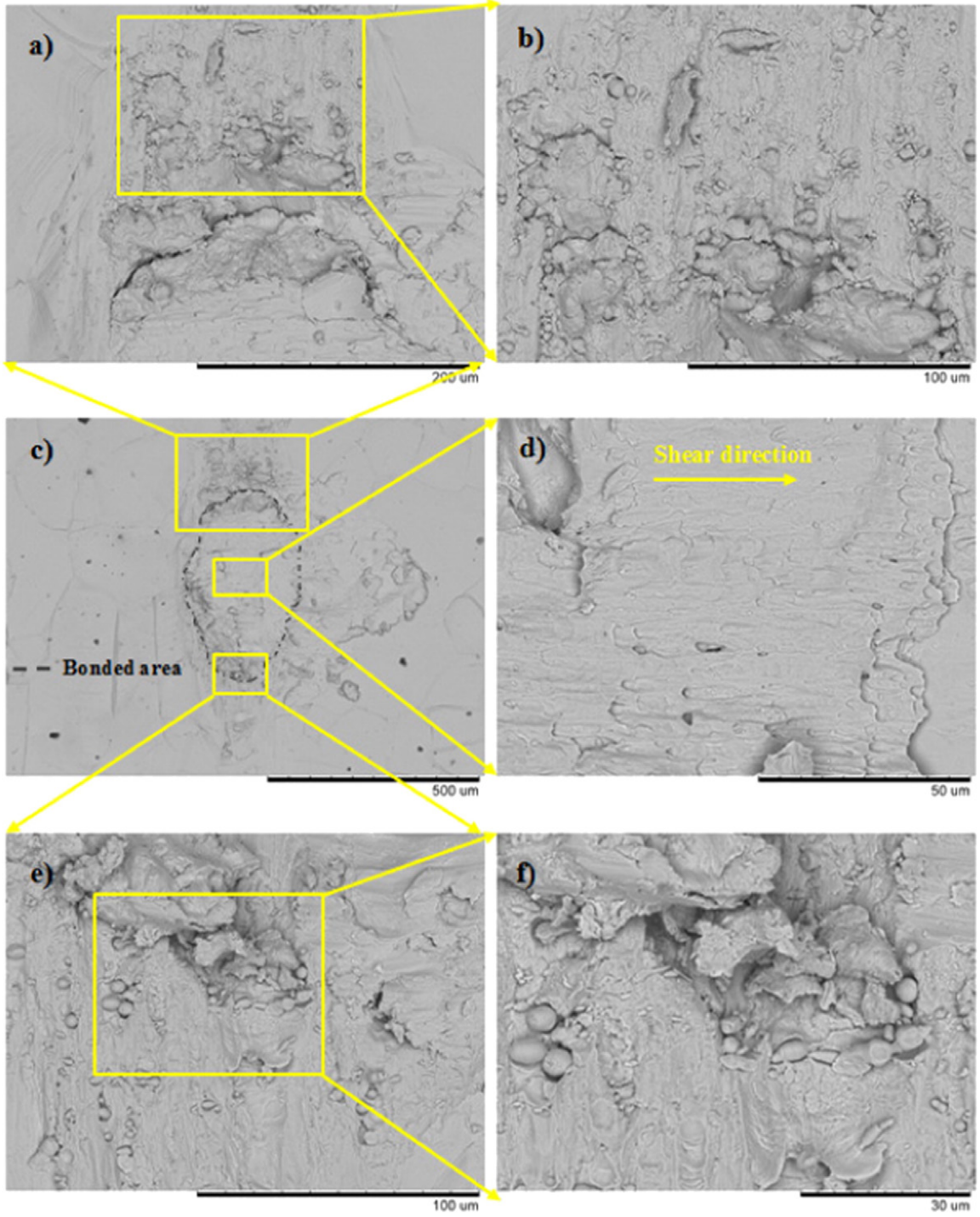

Fig. 7. SEM images showing the morphology of the different regions of a sheared bond surface in the as-bonded condition.

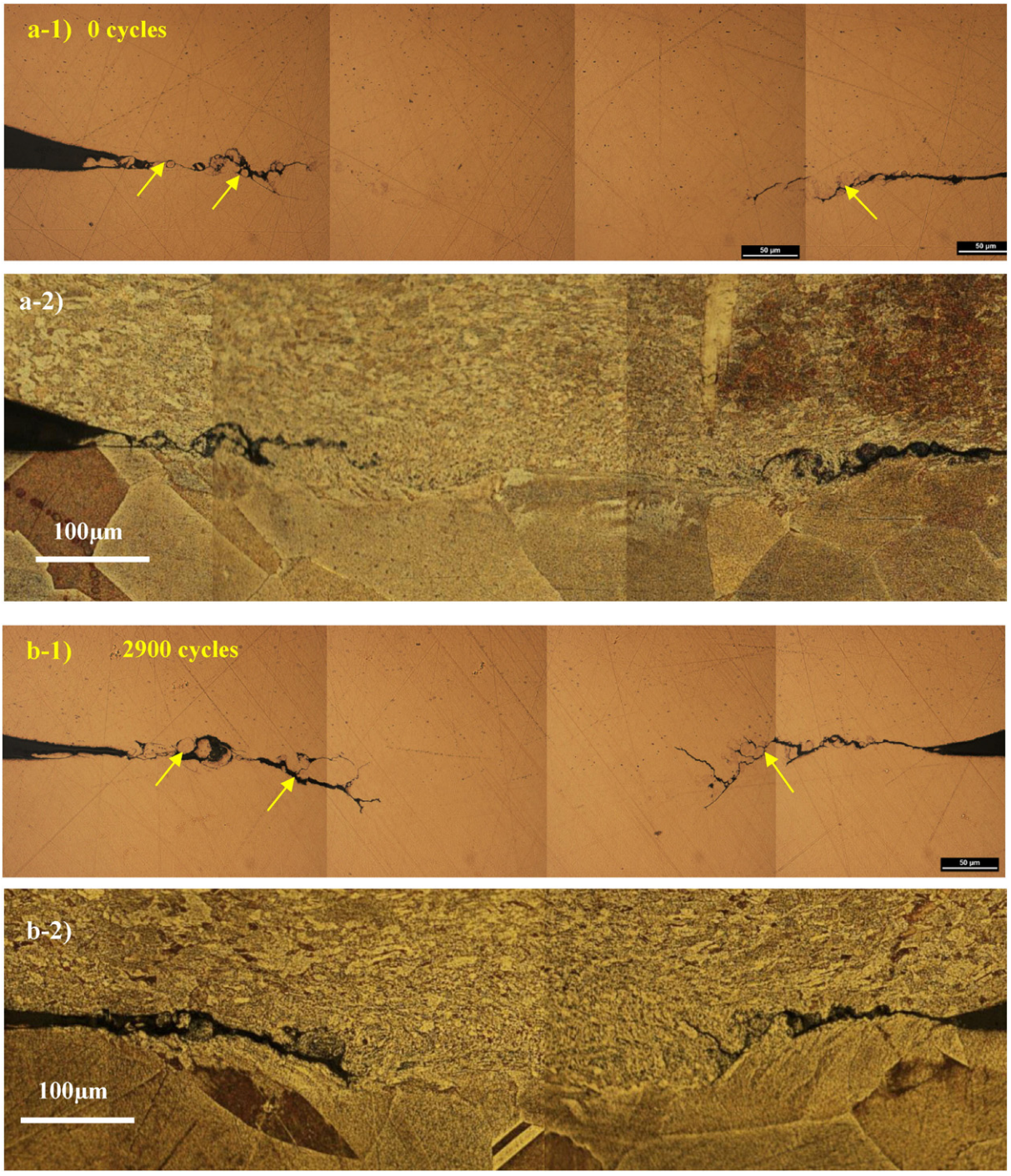

Fig. 8. Cross-sectional view of copper bond interface of a) an as-bonded sample 1) as-polished 2) etched and b) a sample subjected to 2900 thermal cycles, 1) as-polished and 2) etched (two different samples).

Furthermore, spheroid-like particles can again be seen lodged between the pre-cracked interfaces at the extremities of both bonds. These spheroids were not only observed after cycling but also in the as-bonded condition. The origin of these 'spheroids' is as yet unclear and needs more investigation; however they are most probably linked with the ultrasonic bonding process. One possible explanation may be that the scrubbing action of the ultrasonic energy leads to the fragmentation of grains of copper at the interface. In the bonding process, the ultrasonic energy absorbed by the wire significantly reduces its deformation stress, allowing plastic flow to occur at the interfaces and a metallurgical bond to form [15]. These fragmented particles, having absorbed ultrasonic energy, may then adopt a spherical morphology in order to attain a lower energy state. At the same time, these copper particles expose fresh surfaces to oxidation as they break off. SEM EDX analysis of the cross-sections indeed shows these particles to be copper-rich and surrounded by oxygen-rich and carbon-rich phases (see Fig. 9).

The etched optical images (Fig. 8-a2 and b2) and the FIB ion channelling images (Fig. 10-e and f) show the grain structures of the bonds. The grains within the copper layer of the AMB substrate are characteristically large, although the material directly beneath the wedge is severely deformed. In comparison, the wire consists of relatively fine, horizontally deformed grains. The microstructure at the interface is yet finer. After

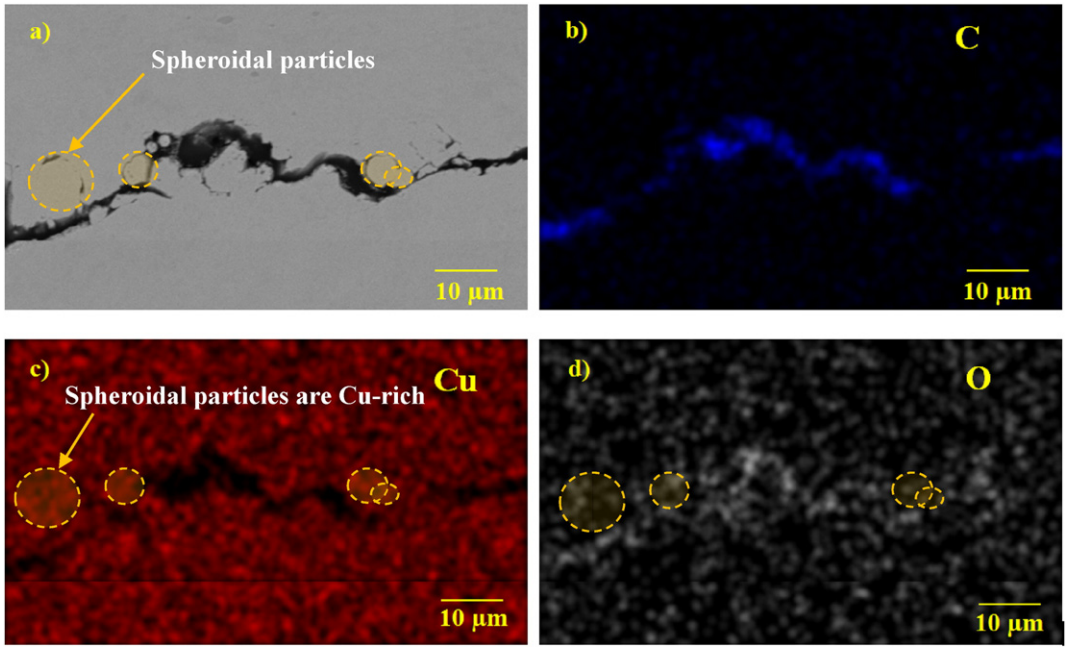

Fig. 9. SEM EDX elemental mapping of a cross-section — after 2900 cycles (a) Electron backscatter image of the interface (b) carbon-rich regions in blue (c) Cu-rich regions in red (d) oxygen-rich regions in white.

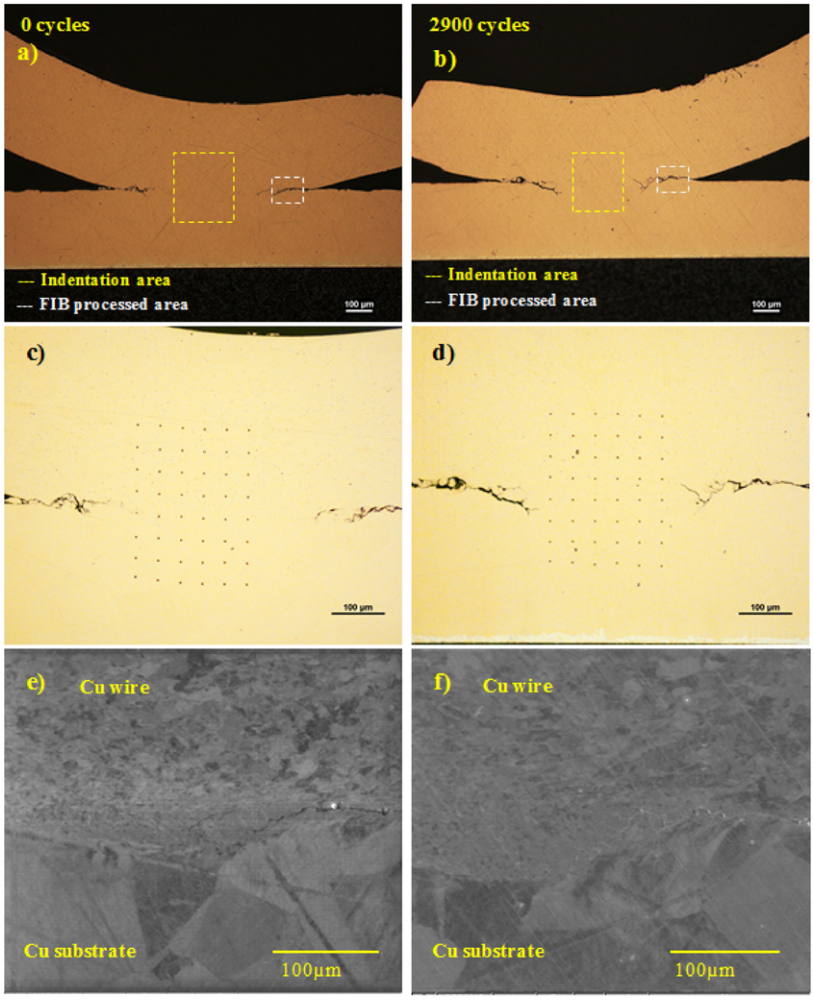

Fig. 10. Cross section view of copper wires in (a) the as-bonded condition, and (b) after 2900 cycles (c) image of nanoindentation test in as-bonded condition, (d) array of indents after 2900 cycles, FIB processed area e) in as-bonded condition and f) after 2900 cycles.

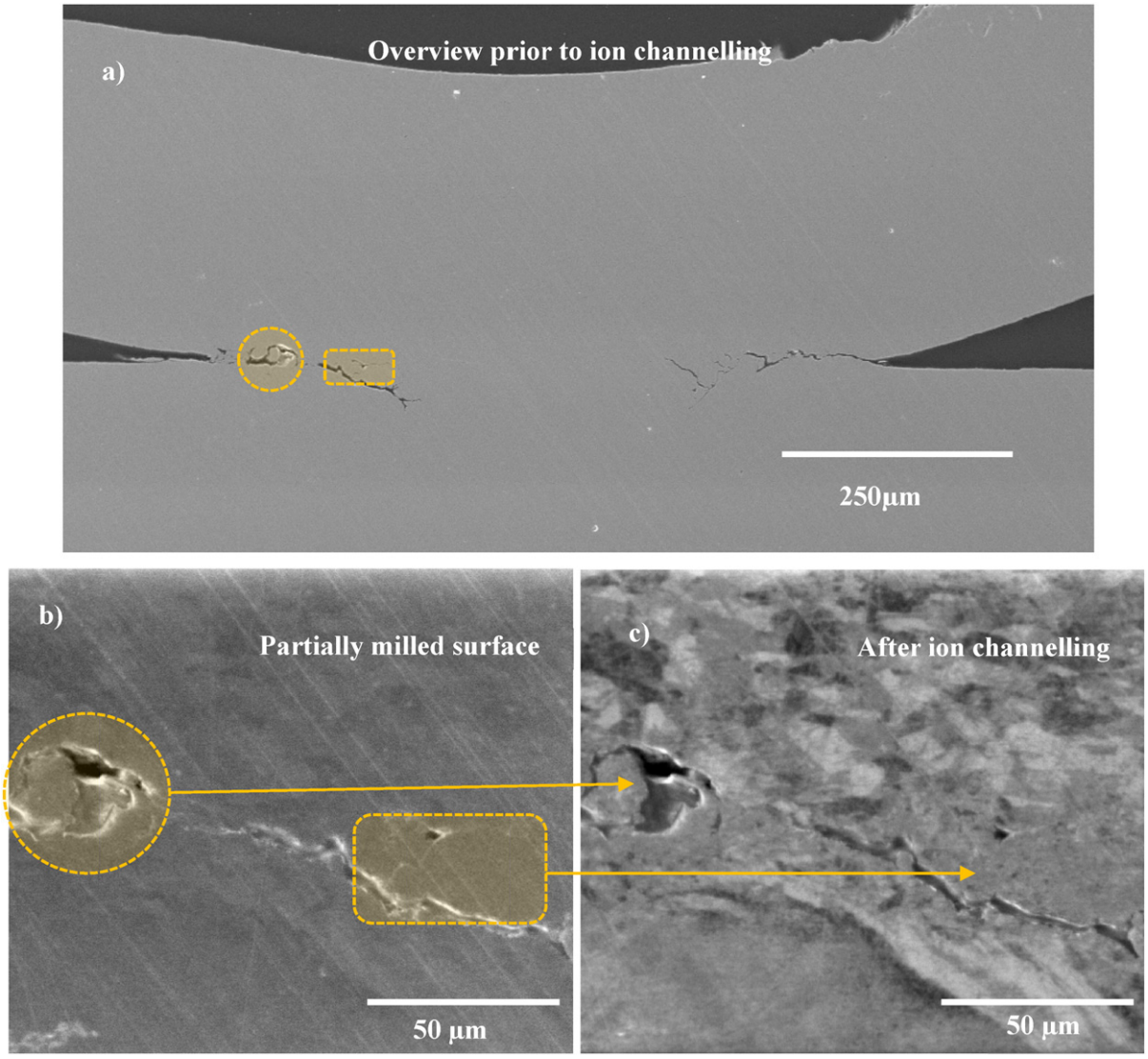

Fig. 11. FIB analysis of round particles.

2900 thermal cycles, little change is discernible in both the wire and the substrate in terms of grain size and morphology (see Fig. 10-f). The FIB images and etched optical micrographs also show that the angle of the pre-crack relates to the bowl-shaped boundary between the wire and the undeformed substrate material directly beneath the wedge. Similarly, the fracture surfaces following shear testing also appear to follow this boundary (see Fig. 6). In addition, FIB images show the Cu-rich spheres discussed previously to contain fine grains similar to those at the interface between the bulk wire and substrate (see Fig. 11); this rules out the likelihood that these spheroidal particles are surface oxide particles.

A row-by-row representation of the results of nanoindentation tests is given in Fig. 12. Overall, indentation hardness values ranged from 1 GPa to 1.8 GPa; this is similar to the results reported by Wiese and Kraemer [16]. It is interesting to note that the substrate undergoes an increase of 22% in indentation hardness which almost matches the increase in shear strength (See Fig. 13) and corresponds to the region of low hardness defining interface between wire and the undeformed substrate. There would also appear to be a slight increase in hardness in the wire. This may possibly be explained by cyclic hardening [16,17]. It is understood that during fatigue, ductile materials undergo an initial stage of cyclic hardening or softening, depending on whether the material is annealed or has been pre-deformed, in that order [17]. This may

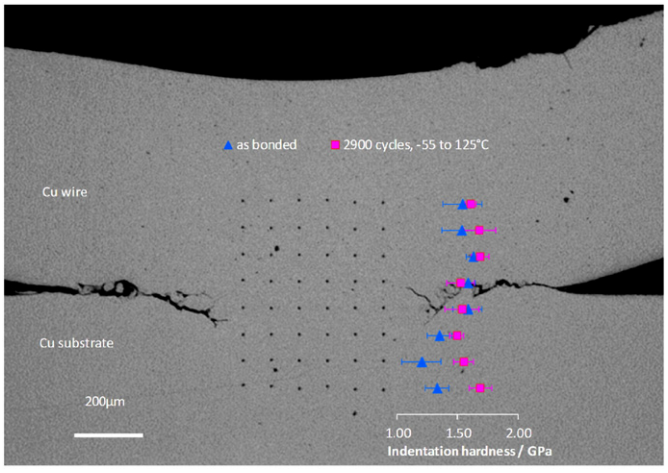

Fig. 12. Representation showing the mean value and spread of indentation hardness per row before and after 2900 thermal cycles.

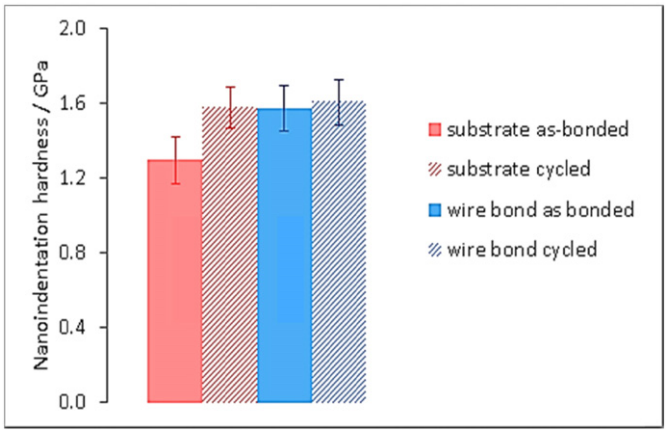

Fig. 13. Nanoindentation hardness results of copper bonds before and after cycling (2900 cycles).

explain why the observed increase in hardness is most pronounced in the substrate, which is in an annealed state as-bonded. The wire material, on the other hand, which is severely deformed, experiences a modest change in indentation hardness. Given the relatively high melting point of copper, it is thought that the processes which drive cyclic softening (dislocation annihilation, grain growth) are insufficient at this number of cycles to offset the initial cyclic strain hardening which takes place under this thermal cycling regime. This may also explain the observation of "increased" shear strength. Thus, the use of shear force measurement in isolation may produce a misleading impression of degradation in such wire bonds.

4. Conclusions

A thermal cycling reliability study of ultrasonically bonded copper wires on AMB Cu substrates are reported in this work. The results obtained from both a non-destructive approach using 3D X-ray tomography and shear tests showed no discernible degradation or wear out from initial condition to 2900 passive thermal cycles from −55 to 125 °C. An apparent increase of shear strength has been observed. Results obtained from nanoindentation showed cyclic hardening that might explain the increase in shear force after cycling. Initial pre-cracks observed underneath the wire occurred at a 45 degree angle to the interface appeared to follow a surface of low hardness defining interface between wire and the undeformed substrate. Further work will aim to characterise any link between this observation and bonding parameters. Further studies are also planned on copper-metalized active devices. Shear test results used in isolation may provide misleading information regarding copper wire bond degradation.

Acknowledgements

The authors gratefully acknowledge the support of the UK Engineering and Science Research Council (EPSRC) through grant EP/I013636/1 (HubNet). The authors are also grateful to Dynex Semiconductors Ltd. for providing AMB cu substrate tiles for this work.

References

[1] R. Bayerer, in: PCIM (Ed.), Higher Junction Temperature in Power Modules – A Demand From Hybrid Cars, a Potential for the Next Step Increase in Power Density for Various Variable Speed Drives, 2008 (Nuremberg, Germany).
[2] M.B. Roland Ott, R. Tschirbs, D.D. Siepe, in: PCIM (Ed.), New Superior Assembly Technologies for Modules With Highest Power Densities, 2010 (Nuremberg, Germany).
[3] A. Syed Khaja, C. Kaestle, J. Franke, Reliable packaging technologies for power electronics: diffusion soldering and heavy copper wire bonding, Electric Drives Production Conference (EDPC), 2013 3rd International, 2013.
[4] K. Guth, et al., New assembly and interconnect technologies for power modules, Integrated Power Electronics Systems (CIPS), 2012 7th International Conference on, 2012.
[5] Buttay, C., et al. Die attach of power devices using silver sintering–bonding process optimization and characterization. In High Temperature Electronics Network (HiTEN). 2011.
[6] D.B. Siepe, Reinhold, R. Roth, The future of wire bonding is? Wire bonding! CIPS 2010, 2010 (Nuremberg, Germany).
[7] F. Hille, et al., Failure mechanism and improvement potential of IGBT's short circuit operation, Power Semiconductor Devices & IC's (ISPSD), 2010 22nd International Symposium on, 2010.
[8] Y. Tian, et al., Investigation of ultrasonic copper wire wedge bonding on Au/Ni plated Cu substrates at ambient temperature, J. Mater. Process. Technol. 208 (1–3) (2008) 179–186.
[9] C. Kaestle, et al., Investigations on ultrasonic copper wire wedge bonding for power electronics, Electronics Technology (ISSE), 2013 36th International Spring Seminar on, 2013.
[10] A. Syed Khaja, et al., Optimized thin-film diffusion soldering for power-electronics production, Electronics Technology (ISSE), 2013 36th International Spring Seminar on, 2013.
[11] C. Kaestle, J. Franke, Comparative analysis of the process window of aluminum and copper wire bonding for power electronics applications, Electronics Packaging (ICEP), 2014 International Conference on, 2014.
[12] H.J. Albrecht, et al., Challenges on diagnostics of power electronics modules and assemblies, Integrated Power Systems (CIPS), 2014 8th International Conference on, 2014.
[13] Gale, W.F. and T.C. Totemeier, Smithells Metals Reference Book (8th Edition). Elsevier.
[14] A. Fischer-Cripps, Critical review of analysis and interpretation of nanoindentation test data, Surf. Coat. Technol. 200 (14) (2006) 4153–4165.
[15] I. Lum, M. Mayer, Y. Zhou, Footprint study of ultrasonic wedge-bonding with aluminum wire on copper substrate, J. Electron. Mater. 35 (3) (2006) 433–442.
[16] S. Wiese, F. Kraemer, Modelling of the mechanical behaviour of copper in 2nd level interconnection structures, Electronics System-Integration Technology Conference (ESTC), 2014, 2014.
[17] H. Mughrabi, Microstructural mechanisms of cyclic deformation, fatigue crack initiation and early crack growth, Philos. Trans. R. Soc. Lond. A Math. Phys. Eng. Sci. 373 (2038) (2015) 20140132.